Rider model for the estimation of tyre forces in off-road motorcycles

Vasquez F.[*a], Lot R.[a], Rustighi E.[b], and Pegoraro R.[c]

[a]*Mechanical Engineering Department, University of Southampton, Southampton, UK SO17 1BJ*
[b]*Institute of Sound and Vibration Research, University of Southampton, Southampton, UK SO17 1BJ*
[c]*WP Suspension, Off-road racing division, Munderfing, Austria*

Abstract

Off-road motorcycles transit over significantly irregular terrains facilitated by their suspension system. The optimisation of their suspension is an open topic. On one hand, on-road motorcycles need to be extended to consider off-road peculiarities such as larger amplitude of motion and a standing rider, to provide optimisation predictions. On the other hand, an objective methodology to verify the predictions is needed since the current practice is to rely on the subjective perception of the rider. In this article, we addressed for the first time, the second problem by developing an estimator of contact forces based on inverse dynamics equations and kinematic measurements. First, in a virtual experiment, it was verified that the estimation is satisfactory. Subsequently, using data recorded at a motocross track, we showed that the estimated forces vary consistently with the obstacles in the track. This provides an objective and consistent indication of the performance of the motorcycle and hence can be used to verify optimisations.

Keywords: Motorcycle Dynamics; Off-Road; Tyre contact force; model-based estimator; rider model;

1 Introduction

Off-road motorcycles are built for commuting, recreation and racing on non-tarmac terrains. These roads usually include significant irregularities and elevation changes. The motorcycle's suspension system partially absorbs impulses from the road [1], making transit on this terrain comfortable and handleable.

The optimisation of the suspension system, as in other vehicles, aims to maximise comfort and/or handling by reducing chassis accelerations and/or enhancing tyre contact forces respectively, [2, 3, 4, 5]. The first approach known to the authors dates from 1983, when Vliet [6] optimised the suspension of an off-road motorcycle by minimising the suspension force and stroke using a one degree of freedom model due to the limited computational power. With the increase in simulation power, more elaborate models have been developed to optimise suspensions of on-road motorcycles. For example, in 2000, Cossalter et. al [7] optimised the suspension of an on-road motorcycle by minimising the braking distance, using a multi-body model with seven degrees of freedom and a rider rigidly attached to the frame. Subsequently, in 2010, Catania et. al [8] optimised the suspension damping using a four degree of freedom model. These models have not been exploited for off-road conditions. Only in 2015, Lozoya et. al [9] studied control strategies to optimise a semi-active suspension in an off-road motorcycle using BikeSim, a professional simulation software. However, passive suspensions, which are predominantly used in production off-road motorcycles, have not been optimised since Vliet.

Current motorcycle models need to be extended to account for off-road peculiarities. For example, larger obstacles and pitch angles, as well as frequent wheel detachments need to be considered. Furthermore, since in motorcycle dynamics, rider's mass contribution to motorcycle-rider system is non-negligible [10], an accurate rider model is also required. On-road and off-road require different models since riding techniques are different. In on-road, the driver is seated, and several models exist to describe his/her lateral motion as a control strategy and some include vertical and horizontal motion as well (see [10] for a review). Contrarily, in off-road driving, the rider is mainly in standing position. In this position, the

---

*Corresponding author: F.A.Vasquez-Stuardo@soton.ac.uk

rider's arms and legs provide significant vibration isolation and hence they should be included as model components [11]. Wilczynski [12] and Wang [11] have developed passive multi-body models of a standing rider to estimate loads on an off-road bicycle. Although the authors [13] proposed a simplified version of those models to estimate off-road motorcycle tyre forces, the problem remains unresolved, since it did not provide good results when tested with experimental data due to omitting the active part of the rider.

The current methodology to setup high performance off-road motorcycle suspensions is by trial and error, using feedback from data acquisition and an experienced test-rider. However, since the rider's feedback is inherently subjective, it does not provide a consistent indication of the motorcycle performance.

Experimental verification of the optimisation requires to measure the variables used as objectives, namely acceleration and/or contact forces. While, measurement of accelerations is straight forward with accelerometers, contact forces are not. In four-wheeled vehicles, direct measurement with wheel force transducer is expensive and used only for vehicle development. As a lower-cost alternative for control applications in production vehicles, estimators of contact forces are used [14]. Regarding two-wheeled vehicles, no force transducer is found in the market. An option is to build a custom-made load cell into the motorcycle parts. This approach requires the reduction of the part's thickness to increase strain and achieve useful sensitivity, which however, is invasive, reduces structural resistance of parts, and in off-road, can endanger the driver due to the high loads involved. As alternatives for control applications, Teerius [15] and Slimi [16] had developed estimators of lateral tyre force for motorcycles. These estimators use kinematic sensors and a kinematic model to estimate lateral tyre slip, which is translated into contact force by a slip-friction tyre model. However, this methodology is intrinsically limited to on-road terrains since tyre models assumes smooth and consistent road characteristics, which is not the case for off-road surfaces.

In summary, optimisation of off-road motorcycle suspensions remains an open issue. On one hand, theoretical models that consider off-road peculiarities are needed to provide predictions and on the other hand, a method to measure contact forces is needed to provide objective verifications.

In this article, we address for the first time the problem of objective verification to avoid rider's perception bias by developing an estimator of contact forces. In section 2, we derive a set of five inverse dynamic equations of the motorcycle, impose a set of constraints to improve the accuracy, and present a novel approximation for the rider forces. In section 3, we present a verification of the estimations using virtual data. In section 4, we show how to treat experimental signals and the results of estimated contact forces in a motocross track. Finally, we discuss limitations and summarize main conclusions.

2 Inverse dynamics method for tyre force estimation

In this section we show how we derived a set of redundant equations to calculate contact forces from kinematic measurements.

The problem of calculating forces from kinematic variables (positions, velocities and accelerations) is referred as inverse dynamics. In addition, if multiple interconnected bodies are involved, it is a multibody problem [17]. Multibody problems can be solved numerically or symbolically. The former strategy, is well suited for final design stages since detailed information is known; while the latter is preferred for early design stages, since it captures the essence of the phenomena [18]. We prefer the second approach since we can additionally manipulate the set of equations to process the experimental data as efficiently as possible. To derive symbolically the equations of motion, we use MBSymba, [18, 19, 20] which is an add-on for Maple [21].

2.1 Equations of motion

The equations of motion of the motorcycle are derived under the following four assumptions. First, we consider in plane motion only, since our interest is mainly on manoeuvres such as braking and accelerating, Figure 1. Second, by neglecting structural vibrations, we can represent the motorcycle by four interconnected bodies with five degrees of freedom, which are described by as many coordinates,

$$\mathbf{q} = [x_s, z_s, \mu, z_f, \alpha_r]^T, \tag{1}$$

where, x_s and z_s are horizontal and vertical displacement of the chassis centre of mass, μ is chassis rotation, z_f is the front suspension compression, and α_r is the rear suspension compression defined as the relative rotation between swingarm and chassis. Third, since the manoeuvres of interest are generally
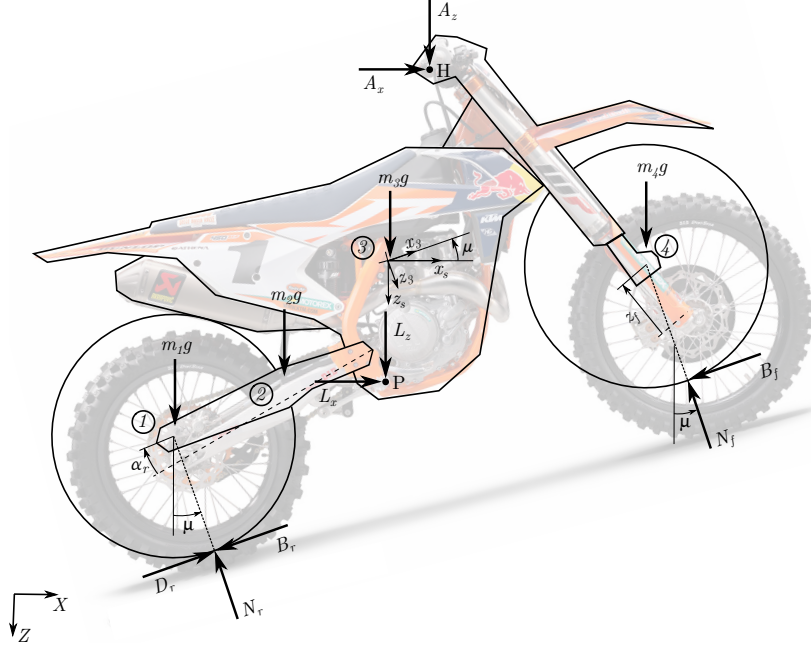
Figure 1: Motorcycle model. x_s, z_s and μ are horizontal, vertical and angular position of chassis centre of mass; z_f is fork compression, and α_r is swing arm angular compression; A_x, A_z, L_x, L_z are rider's arm and leg forces acting over the handlebar (H) and foot-peg (P); N_r and N_f are normal forces over the tyres assumed to be along the z_3, which is tilted μ from absolute vertical; B_r, B_f are rear and front braking force and D_r is rear driving force which are assumed to be along chassis x-axis.

transited in standing position, we consider that the rider interacts with the handlebar and foot pegs only. Fourth, the contact point with the ground is considered to be directly under the wheel centre as seen in nominal condition. This implies that the contact point does not move forward or backwards due to road irregularities, and therefore, normal and tangential components are always aligned with z_3 and x_3 axis, respectively. This simplification is based on the observation that only when transiting large obstacles, such as *whoops*, Figure 2, the contact points move significantly from the bottom of the tyres. In this way, the estimation of the contact point position, which is not a trivial task, is avoided and there are only four tyre force components to be determined.

We derive five equations of motions, one for each degree of freedom, and collect them as

$$\mathbf{M}\ddot{\mathbf{q}} + \mathbf{m_v} = \mathbf{A_w}g + \mathbf{A_s}\mathbf{f_s} + \mathbf{A_r}\mathbf{f_r} + \mathbf{A_t}\mathbf{f_t}, \tag{2}$$

where, $\mathbf{M}$ is the mass matrix, $\ddot{\mathbf{q}}$ is the acceleration vector, g is gravity acceleration, $\mathbf{f_s}$, $\mathbf{f_r}$, $\mathbf{f_t}$ are suspension, rider and tyre force vectors respectively and the matrices $\mathbf{A_w}$, $\mathbf{A_s}$, $\mathbf{A_r}$, $\mathbf{A_t}$ project these forces along each of the five coordinates. $\mathbf{m_v}$ is the pseudo-mass vector which contains relative acceleration terms, and also the product of wheels rotational inertia by their angular accelerations. We did not model wheel rotations as coordinates in $\mathbf{q}$ since we can measure them directly to represent the rotational inertia effect and therefore, we did not need to derive equations of motion for them. See Appendix A, for explicit description of matrices and vectors.

In Equation (2), masses , rotational inertias, and geometry in $\mathbf{M}, \mathbf{m_v}$ and projection matrices can be measured with no major complication. Accelerations in $\ddot{\mathbf{q}}$, velocities and angular acceleration in $\mathbf{m_v}$, and positions can be measured with accelerometers, potentiometers and tachometers or derived from them; suspension forces $\mathbf{f_s}$ can be estimated from characterisation of the spring and damper; and the rider forces $\mathbf{f_r}$ can be estimated as described on Section 2.4.

2.2 Tyre force estimation

Acknowledging the presence of measurement errors, we decide to derive an overdetermined system to reduce them. In particular, Equation (2) consist on five equations to determine four unknown tyre force components. Because of the presence of random errors in the equations, there is no vector $\mathbf{f_t}$ that can

Table 1: Known tyre forces under specific driving conditions. The auxiliary weights w_f, w_r and w_d represent front and rear wheel detachments and motorcycle driving (accelerating), respectively. They are 1 if the condition is happening and 0 otherwise, and are used to calculate the constraint activation weights W_{ii}. The symbol - means that it can be any value.

Tyre force		Magnitude in driving condition				Constraint activation
		Front	Rear	Driving	Braking	weight
i	$f_{t,i}$	detached	detached	$(w_d = 1)$	$(w_d = 0)$	W_{ii}
		$(w_f = 1)$	$(w_r = 1)$			
1	N_f	0	-	-	-	w_f
2	N_r	-	0	-	-	w_r
3	B_f	0	-	0	-	$w_d + w_f - w_d w_f$
4	B_r	-	0	0	-	$w_d + w_r - w_d w_r$
5	D_r	-	0	-	0	$(1 - w_d) + w_r - (1 - w_d)w_r$

satisfy the five equations simultaneously. Then, the alternative problem is,

$$\text{find } \mathbf{f_t} \text{ that :}$$
$$\min_{\mathbf{f_t}} \ \|\mathbf{A_t f_t} - \mathbf{b_1}\|, \tag{3}$$

where, $\mathbf{b_1} = \mathbf{M\ddot{q}} + \mathbf{m_v} - \mathbf{A_w}g - \mathbf{A_s f_s} - \mathbf{A_r f_r}$, is the vector of known terms of Equation (2).

The overdetermined system can not compensate the measurement errors completely and non-physical solutions can be obtained regardless. To reduce these non-physical solutions, we add equality and inequality constraints to the optimisation.

On one hand, we add inequality constraints to consider that normal forces and front tangential force (braking) can physically exist in one direction only. By defining the rear tangential force as two non-negative forces as well, we add the constraints,

$$\mathbf{f_t} = [N_f \ N_r \ B_f \ B_r \ D_r]^T \geq \mathbf{0}, \tag{4}$$

where, N_f and N_r are normal forces on front and rear tyres; B_f and B_r are braking forces on front and rear tyre; and D_r is the driving force on the rear tyre. Even though in this way there are five variables to be determined, the problem still has four unknowns, since by definition only D_r or B_r exist at anytime.

On the other hand, we add equality constrains to impose a solution when some terms are known under certain driving conditions. These are: $N_f = B_f = 0$ when front wheel is detached; $N_r = B_r = D_r = 0$ when rear wheel is detached; $B_f = B_r = 0$, when motorcycle is driving (accelerating); and $D_r = 0$ when braking, Table 1. In order to impose these constraints only under the corresponding conditions, we multiply each constraint equation by an activation weight, W_{ii}, that is 1 when the condition is satisfied, and 0, otherwise. In this way, we express the constraints as

$$\mathbf{W f_t} = \mathbf{0}, \tag{5}$$

where $\mathbf{W} = \text{diag}(W_{ii})$.

To make $W_{ii} = 1$ under the corresponding driving conditions, we define three auxiliary weights, w_f, w_r and w_d, representing the conditions for front wheel detached, rear wheel detached, and motorcycle driving, respectively. They take the value of 1 if the corresponding condition is happening, and 0 if not. Next, we read Table 1 horizontally to identify under which conditions the tyre force i is null, and therefore, W_{ii} needs to be 1, to activate the constraint. In particular, since each normal force is null only under one condition, by making the activation weight W_{ii} equal to the weight representing the condition, it will be 1 only under that condition. Differently, the tangential forces can be null under two conditions. To make the activation weight W_{ii} equal to 1 if any of the two or both conditions are happening, we add the weights representing the conditions and subtract their product, which is the algebraic representation of an *or* logical condition. In this way, the activation weights $W_{11}, ..., W_{55}$ are obtained and shown on Table 1.

With these constraints, some non-physical combinations are implicitly removed, such as tangential forces combined with no normal forces. Additionally, in this formulation, three driving possibilities have

been omitted as well. These are, driving and braking simultaneously, front wheel driving, and no driving nor braking. The first, since it is not expected in normal driving conditions; the second, since front wheel drive motorcycles are very rare; the third, since it is only possible in still condition, which is out of interest. When there are no inputs from the rider to drive or brake, which apparently classifies as the third case, actually involves braking because of friction between moving parts.

The imposition of a solution when some terms are known under certain driving conditions could have been done by removing the known terms from the system in stead of adding constraints to the system. However this approach requires to reduce the system of Equation (3), into $\min \|\mathbf{A_t'}\mathbf{f_t'} - \mathbf{b_1'}\|$ for the six driving conditions which are possible: only braking, only driving, driving or braking with front wheel detached, braking with rear wheel detached, and both wheels detached. Even though this option solves a smaller system which would make it faster, we prefer adding the constraints, since numerical implementation is simpler, and the additional calculation time is not significant.

Adding the constraints, the problem is now formulated as

$$
\begin{aligned}
&\text{find } \mathbf{f_t} \text{ that :} \\
&\quad \min_{\mathbf{f_t}} \ \|\mathbf{A_t}\mathbf{f_t} - \mathbf{b_1}\|, \\
&\text{subject to: } \quad \mathbf{f_t} \geq \mathbf{0} \\
&\qquad\qquad\quad \mathbf{W}\mathbf{f_t} = \mathbf{0}.
\end{aligned}
\tag{6}
$$

2.3 Weighted system and solution

In order to solve the problem efficiently, we transform it to

$$
\begin{aligned}
&\text{find } \mathbf{f_t} \text{ that :} \\
&\quad \min_{\mathbf{f_t}} \ \|\mathbf{B}(\mathbf{A}\mathbf{f_t} - \mathbf{b})\|, \\
&\text{subject to: } \quad \mathbf{f_t} \geq \mathbf{0},
\end{aligned}
\tag{7}
$$

where,

$$
\mathbf{B} = \begin{bmatrix} \mathbf{B_d} & \mathbf{0} \\ \mathbf{0} & \mathbf{B_c} \end{bmatrix}, \quad \mathbf{A} = \begin{bmatrix} \mathbf{A_t} \\ \mathbf{W} \end{bmatrix}, \quad \text{and} \quad \mathbf{b} = \begin{bmatrix} \mathbf{b_1} \\ \mathbf{0} \end{bmatrix}.
\tag{8}
$$

which is a non-negative least squares problem, to apply the Lawson-Hanson algorithm for non-negative problems, presented in [22], and implemented in MATLAB [23] as `lsqnonneg`.

To perform this transformation, first, we take advantage that the minimisation argument is in least squares form which enables us to use least squares solvers. These solvers are considerably faster than other optimisation solvers since they exploit the particular formulation. Specifically, to solve an equality constraint least squares problem, as the one in Equation 6, there are at least four algorithms. Lawson and Hanson [22] describe three: by using a basis of the null space, by direct elimination, and by weighting, while MATLAB uses by default interior-point-convex algorithm. We chose to solve the problem by weighting, which means appending the equality constraints $\mathbf{W}\mathbf{f_t} = \mathbf{0}$ to the minimisation argument with a heavy weight, which we do with the diagonal matrix $\mathbf{B_c}$. The main difference with this formulation is that the constraints are not exactly met, which for this situation is beneficial since it helps to compensate for errors in the transitions between active and inactive constraints.

Additionally in this transformation, we weight the dynamic equations $\mathbf{A_t}\mathbf{f_t} - \mathbf{b_1} = \mathbf{0}$ by diagonal matrix $\mathbf{B_d}$. This is to take into account the difference in uncertainties that might exist between equations given that they are obtained from different measurements.

2.4 Rider forces

The forces between the motorcycle and the rider in standing position, namely, at hands and feet, are the result of passive and active actions of arm and leg muscles and tissues, commanded by conscious and unconscious decisions of the rider. Prediction of these forces by approximating the rider as a multibody system and muscle forces as passive elements, excited by chassis motion, is inaccurate because of the lack of adequate rider parameters and the omission of active components [13]. Moreover, it is computationally expensive since a differential equation of motion needs to be integrated. An alternative, is to measure the torso kinematics to estimate the forces by inverse dynamics. This approach involves attaching sensors to the rider and wire them to the chassis which we prefer to avoid since it creates a potential risk in
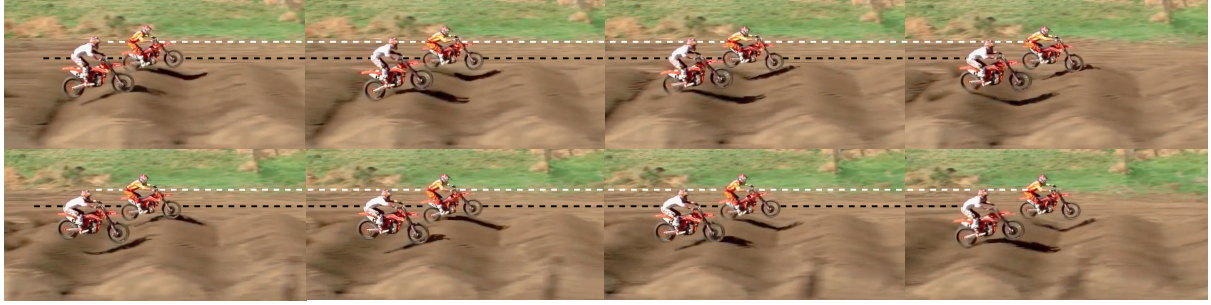
Figure 2: Two motorcycles riding through *whoops* section. It shows that although the riders moves broadly, the vertical position of their hips shown in white and black dashed lines, remains roughly at the same height [25].

case of a fall. A wireless option could be implemented based the work of Cheli *et. al* [24] who developed a system that uses a camera mounted on the tail of the motorcycle and a target on the rider's back to measure his/her position. However, this approach would require a double numerical differentiation, that inherently propagates errors, to retrieve accelerations, which are the predominant inputs for inverse dynamics calculations. Consequently, we prefer to develop a simple model in first instance, and in a second stage, develop a more sophisticated methodology to measure rider forces.

To estimate the fundamental characteristics of the rider forces, we take into consideration two situations. First, observation of the rider driving in irregular roads, shows that the centre of gravity, which is approximately in the hip, is almost on a constant vertical position (Figure 2), therefore velocity and acceleration are small, which implies that arm and leg vertical forces are close to equilibrium with rider's weight, and consequently, are close to constant.

Second, in braking and acceleration, his/her centre of mass barely moves horizontally with respect to the chassis, which implies that their horizontal accelerations should be similar. Consequently, the total vertical and horizontal forces over the rider can be approximated as the weight and the horizontal inertial force, respectively. In order to further simplify the representation, we assume that the vertical force is completely exerted through the legs, and the horizontal, by the arms, resulting in

$$\mathbf{f_r} = [L_x \ L_z \ A_x \ A_z]^T = [0 \ m_r g \ -m_r \ddot{x}_s \ 0]^T. \tag{9}$$

Lastly, we consider that all components are zero if contact is lost in front and rear wheels simultaneously.

3 Verification by Simulation

The estimator and the rider model are first tested using data from a virtual experiment, since measurements are noise free and it is possible to measure the contact forces directly. To this end, a motorcycle is modelled in Working Model 2D [26], and a passive rider is considered to generate forces different from the rider model. The passive rider consist on a point mass, translating in the plane, located nominally over the foot-peg and rearwards of the handlebar, and attached to these points by spring and damper elements. Four tests are carried out where the motorcycle states are measured and passed to the estimator to calculate tyre forces which are compared to the forces measured directly in the virtual simulation.

In particular, on the first test, 120 Nm of braking torque are applied on the rear wheel and subsequently on the front wheel, to check if the estimator distinguish the origin of the braking force. On the second test, 60 Nm of braking torque are applied on each wheel simultaneously, to check if the estimator can identify the braking distribution between wheels. On the third test, 120 Nm of driving torque are applied on the rear wheel via shaft drive transmission, to compare with the the fourth test, in which 119.4 Nm of driving torque are applied on the rear wheel via chain transmission, to check the effect of neglecting the chain tension on the estimator. Additionally, in the four tests, the estimation of normal forces is checked.

The inputs for the estimator are as follows. The rider is considered as on section 2, and the suspension forces are linear as on the virtual model. The weights considered in **B** are 1 for the dynamic equations, since they are noise free, and 100 for the constraint equations, to force the constraints to be met.

Figure 3, shows the estimated forces for the braking tests. On test 1, it can be seen that the estimator is able to recognize which wheel is originating the braking force and also provide a close estimate of the
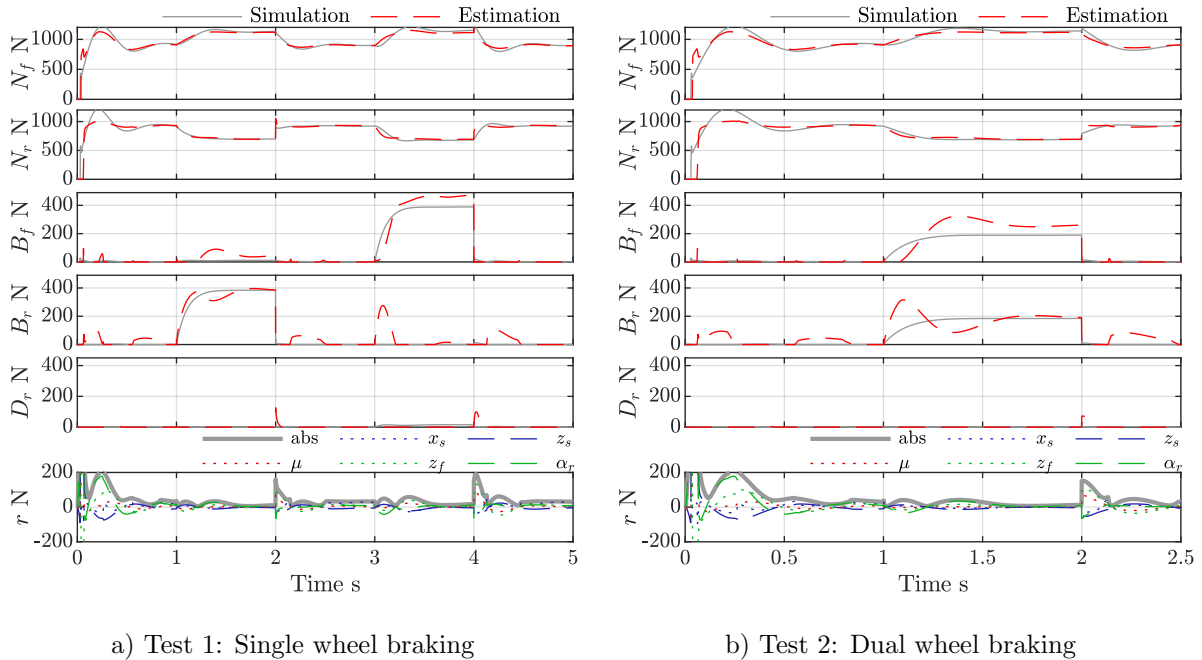
a) Test 1: Single wheel braking   b) Test 2: Dual wheel braking

Figure 3: Braking tests. On both tests 120 Nm of braking torque are applied. In the first test it is first applied to rear wheel on time interval $t = [1\ 2]$ s and then to front wheel on $t = [3\ 4]$ s, and on the second is split equally between front and rear wheel.

magnitude, though front braking is slightly overestimated. On test 2, it can be seen that it recognizes that both wheels are braking, but the braking distribution is estimated inconsistently. Specifically, first, it estimates more to the rear, subsequently, more to the front, and then stabilizes, with front braking slightly overestimated.

Figure 4, shows the estimated forces for the driving tests. It can be seen that in both tests the magnitude of the driving force is closely estimated, and no significant difference is seen if the motorcycle is shaft- or chain-driven. This implies that neglecting chain tension does not add significant error.

Normal forces are satisfactorily predicted on the four tests. Load transfer to the front wheel when braking, and to the rear while accelerating are clearly recognized by the estimator.

Checking the residuals, it can be seen that in test 3, when driving torque is being applied, between seconds 1 and 2, the residuals in the five equations are close to null as expected, since the transmission is the same in the virtual and estimator models. Contrarily, on test 4, the residuals are important since the chain tension is missing in the estimator. Specifically, there is a significant positive residual in the rear suspension compression equation normalized by its length (α_r/l_r), and also, a negative residual of the pitch equation normalized by wheelbase (μ/w). The sign of these residuals are consistent with the chain tension absence, because by pulling between rear wheel and chassis, the chain produces a negative torque over the rear wheel and swing arm, and as a reaction, a positive one over the chassis, both of which are absent on the equations. Accordingly, if a positive torque is added to the pitch equation, and a negative torque to the swing arm equation, it would bring the residuals back to null.

In summary, in the four tests, the estimated forces are in good correspondence with the virtual experiment. The magnitudes and origin of braking forces and driving force are satisfactorily detected, as well as the normal forces. Additionally, it was shown that the omission of the chain tension in the estimator does not affect significantly the prediction of the driving force. Furthermore, the passive rider model used in the virtual experiment served to illustrate that different rider forces over the motorcycle as the one assumed by the estimator do not influence significantly the estimation.

4   Experimental verification

In this section, we test the performance of the estimator and the rider model with experimental data collected with an instrumented motorcycle driven by a professional driver on a motocross track. First, we describe how to obtain the input variables for the dynamic equations as well as the activation weights
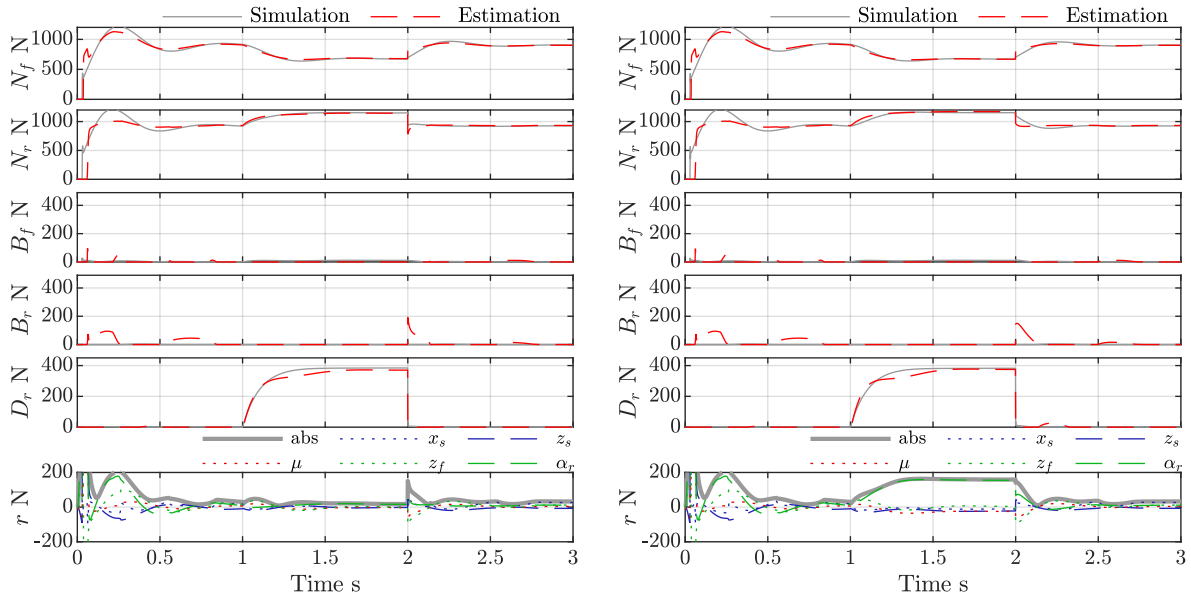
a) Test 3: Shaft drive motorcycle

b) Test 4: Chain drive motorcycle.

Figure 4: Driving tests. On test 3, 120 Nm are applied directly to the rear wheel via a shaft drive transmission, while on test 4, 119.4 Nm are applied to the rear wheel via chain drive transmission, which is driven by an engine torque of 38 Nm. Chain drive transmission ratio is 3.14.

for the constraints from the measuring system. Subsequently, we discuss the estimated forces along the motocross track as well as possible improvements.

4.1   Data collection and preprocessing

The motorcycle used is a 2017 motocross motorcycle fitted with the suspension behaviour depicted in Figure 5. The test is performed on a motocross track which consists on nine straights and nine turns, Figure 6. Straights one, seven and eight (S1, S7 and S8) consist on a sequence of jumps and straight six, consist on *whoops*, which is a sequence of medium size bumps similar to Figure 2. Five laps are recorded, each of which is done in approximately 55 s, and number lap four is picked randomly for the analysis .

The dynamic equations derived in section 2 require fifteen variables to compute the tyre forces. Of those, we measure eight variables with commonly available sensors, while the remaining seven are calculated from the measured ones by numerical integrations or differentiations. Numerical integrations are performed by trapezoidal method with previous removal of signal mean to avoid drift, and differentiations are performed by a finite impulse response filter with delay compensation. The source of each variable is detailed in Table 2.

The sensors used are as follows. An inertial unit is located under the seat from which vertical acceleration of the chassis, pitch angle and forward velocity (from GPS) are obtained. Accelerometers on steering head and tail, aligned with z_3 axis are used to compute pitch angle acceleration as the ratio between the difference measured by them and their distance. On the front suspension, a potentiometer aligned with the fork measure position, and accelerometers at both ends of the fork and aligned with it, are used to compute the compression acceleration, as the difference measured by them. Similarly, on the rear spring-damper unit ('shock') a potentiometer and accelerometers at each end aligned with it, measure its position and acceleration, respectively. Then these signals are translated to rear suspension compression angle using a previously measured relationship between shock position and relative angle between chassis and swing arm, see [1] for details of the procedure. Wheel rotational velocities are not variables of the estimator, but are measured by tachometers to calculate rotational accelerations. One signal per coordinate is shown in Figure 7.

The signals are filtered by a perfect bandpass filter. It consists on a a fast Fourier transform to remove the unwanted components on the frequencies domain, followed by an inverse fast Fourier transform to get the filtered time-domain signal. Two low cut-off frequencies are used. On positions and forward velocity, it is the lowest positive frequency, to maintain the signal mean which physically exists on them,
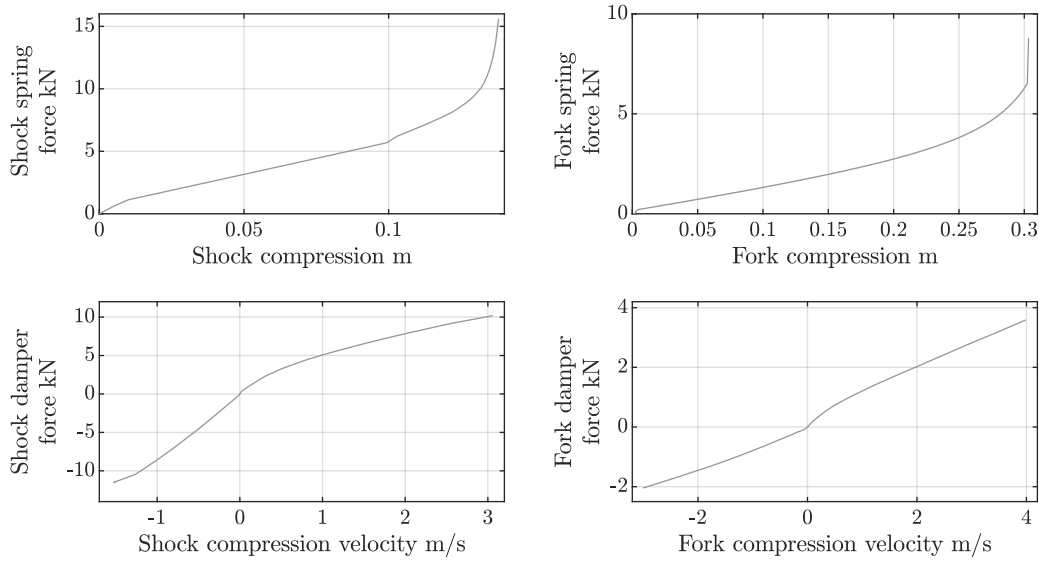
Figure 5: Shock and fork elastic and damping forces used on the tests

Figure 6: Trajectory on the track as measured by GPS. There is a discrepancy on straight 6 (S6) because the track was modified between the picture was taken and the test was performed.

Table 2: Source of variables for the dynamic equations. Eight variables are measured with commonly available sensors while the remaining seven are calculated by numerical differentiation o integration of the measured ones. Wheel rotation velocities are not variables of the estimator, but are the source of rotational accelerations.

| Coordinate		Position	Velocity	Acceleration
Chassis horizontal displ.	x_s		GPS	$\frac{d\dot{x}_s}{dt}$
Chassis vertical displ.	z_s		$\int \ddot{z}_s dt$	Accelerometer
Chassis pitch angle	μ	Inclinometer	$\int \ddot{\mu} dt$	2 Accelerometers
Front suspension compr.	z_f	Potentiometer	$\frac{dz_f}{dt}$	2 Accelerometers
Rear suspension compr.	α_r	Potentiometer	$\frac{d\alpha_r}{dt}$	2 Accelerometers
Front wheel rotation	μ_4		(Tachometer)	$\frac{d\dot{\mu}_4}{dt}$
Rear wheel rotation	μ_1		(Tachometer)	$\frac{d\dot{\mu}_1}{dt}$
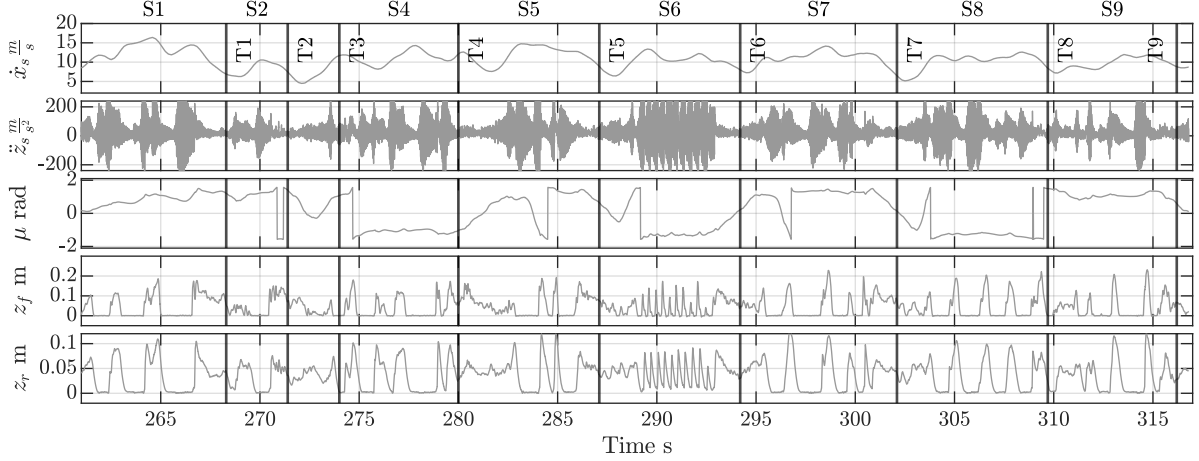
Figure 7: Five measured signals on a lap. Forward velocity, vertical acceleration, pitch angle, fork and shock compressions. T1-T9 provide guidance to relate the measurements with obstacles in the track. Yellow line over the track represents the trajectory measured by GPS. There is a discrepancy on straight 5 (S5) because the track was modified between the picture was taken and the test was perfomed.

while on the rest, is set to zero, since if a mean exists, is due to noise. As high cut-off frequency, 20 Hz is used to remove engine structural vibrations.

In order to detect the three driving conditions in which part of the solution is known for the activation weights, the available sensors are used. On one hand, driving (accelerating) is detected directly by the horizontal acceleration of the chassis. On the other hand, wheel detachment cannot be detected directly with the available sensors, and it is approximated by the suspension strokes, since full extension is reached when the wheel is on the air. The limitations of this approximation are the instants right after detachment and right after contact recovery. The former, since it takes some time to the suspension to reach full extension due to damping, and the latter, since a minimum force is required to begin compression due to stiction.

Two rules are defined to determine if the condition is happening. On one hand, motorcycle is driving if the horizontal acceleration is positive. On the other hand, wheel had detached from the ground if the corresponding suspension compression is reduced under a threshold, Figure 8. Since the three signals used for the detection are not just 0 and 1, their magnitude are mapped into the interval [0 1], using the saturation function

$$\text{sat}(y, y_0) = \frac{1 + \sin(\text{atan}(y/y_0))}{2} \tag{10}$$

which behaves as a step function, resulting in 0 if the argument y is negative, and 1 if it is positive. The function has a smoothed transition between 0 and 1 which is controlled by the parameter y_0. To illustrate this transition, some outputs in the vicinity of $y = 0$ are provided: $\text{sat}(-y_0, y_0) \approx 0.15$; $\text{sat}(0, y_0) = 0.5$; and $\text{sat}(y_0, y_0) \approx 0.85$.

In this way, the three auxiliary weights, w_f, w_r and w_d are calculated as:

$$\begin{aligned}
w_d &= \text{sat}(\ddot{x}_s, \ \ddot{x}_{s,sat}), & 1, \ &\text{if motorcycle is driving;} \\
w_f &= \text{sat}(-z_f + z_{f,min}, \ z_{f,sat}), & 1, \ &\text{if front wheel lost contact;} \\
w_r &= \text{sat}(-\alpha_r + \alpha_{r,min}, \ \alpha_{r,sat}), & 1, \ &\text{if rear wheel lost contact.}
\end{aligned} \tag{11}$$

Lastly, the weights in $\mathbf{B_d}$ are set to 1 as default value, and $\mathbf{B_c}$ are set to 100, to force the constraints to be met.

4.2 Analysis of estimated contact forces

Using the estimator proposed in section 2 together with kinematic measurements treated according to section 4.1, we are able to provide, for the first time, an estimation of the contact forces generated by an off-road motorcycles in real driving conditions, which are shown in Figure 9.

The estimated forces vary consistently with the obstacles of the track. Zones of jumps, braking and acceleration can be clearly recognized from the forces. For example, three jumps can be identified on S1.
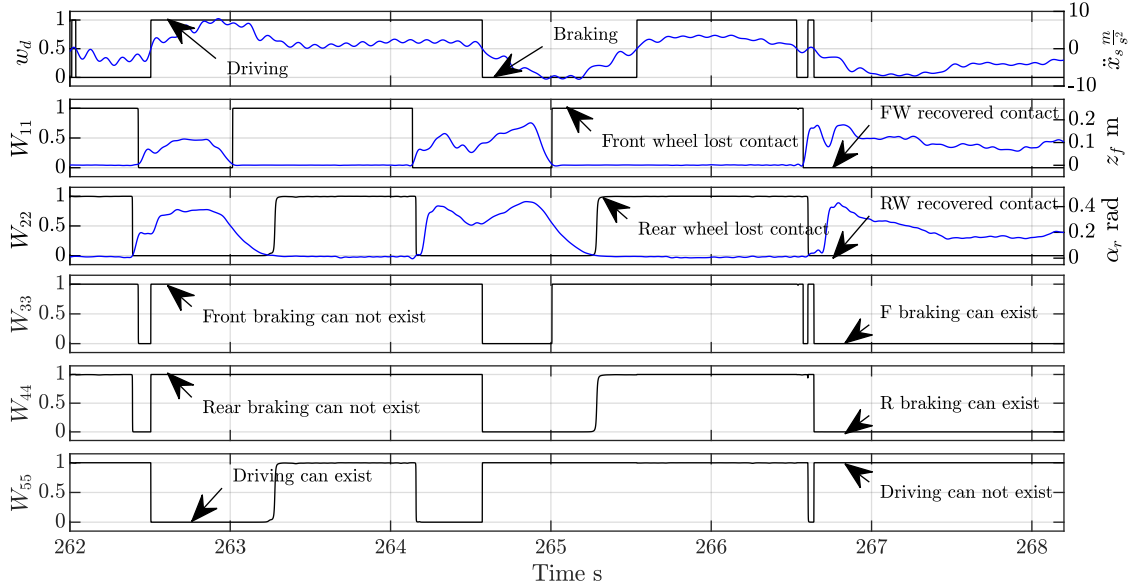
Figure 8: Auxiliary weights w_d, w_f and w_r record the occurrence of driving, front, and rear wheel detachments, based on horizontal acceleration, front, and rear suspension compression, respectively. Weights W_{11} to W_{55} are obtained according to Table (1)

.

There are three absence of forces, showing that the motorcycle is flying, and in between them, normal and driving forces showing that as soon as it lands, it throttles for the next jump. After the third jump, braking forces can be seen in both wheels, which shows that the brakes are applied just after landing, and after the turn, the driving force to exit the turn is also depicted. A similar pattern can be recognized on S7 and S8. On S6, the transit over the *whoops* can be clearly identified by the variation on the normal forces. On S4 and S5, large jumps can be identified as relatively long absence of forces.

Furthermore, taking a closer look into the normal forces, Figure 10, it is possible to distinguish short detachments, for example in the rear wheel while braking before T6. This is of interest for the optimisation, since if these detachments are reduced a harder braking could be possible.

In Figure 10 it is also possible to observe a rear braking force in the middle of the *whoops* section. In this section, the bumps get between the front and rear wheels, creating a normal force tilted backwards, and not aligned with z_3 axis as assumed by the estimator. Nonetheless, the horizontal component of this force reduces the speed of the motorcycle and is detected as a braking force. The detection of this braking is also of interest for the optimisation, since it creates an unwanted braking.

When comparing these forces with preceding and subsequent laps on the test (not shown here), the same pattern of forces is seen. Small variations such as number of detachments in braking or magnitude of peaks in landings, show that variations in driving along tests can also be distinguished.

The residuals of the estimation $\mathbf{r} = \mathbf{B}(\mathbf{A}\mathbf{f_t} - \mathbf{b})$ are depicted in Figures 9 and 10. Peaks around landings and high impacts zones shows that in these parts the estimator's assumptions diverge from reality. From the four assumptions of the dynamic equations and the simplifications of the rider model, the most feasible cause is the assumption of constant vertical force of the rider since it is unlikely that the rider can absorb perfectly the impacts. Contrarily, around turns, as seen in Figure 10, the residuals are not high, indicating that the estimator assumptions are in better agreement with reality. Additionally, it can be seen that the residuals are of similar magnitude, indicating that no equation is dominating the errors.

These results show that the estimated forces vary consistently with the obstacles of the track and therefore are able to provide an objective measurement to verify optimisations. Moreover, it is shown that it can provide additional valuable information for the optimisations such as detachments, *whoops* braking and variations in driving along tests. Furthermore, since this information is derived from objective measurements, it is free from rider's bias and is reproducible.

The magnitudes of the estimated forces should be taken only as a reference, and focus on the variations. This is because the precision of the estimation was not determined, since it was not feasible, in practice, to measure the contact forces with the envisaged methodology. Apart from validating the
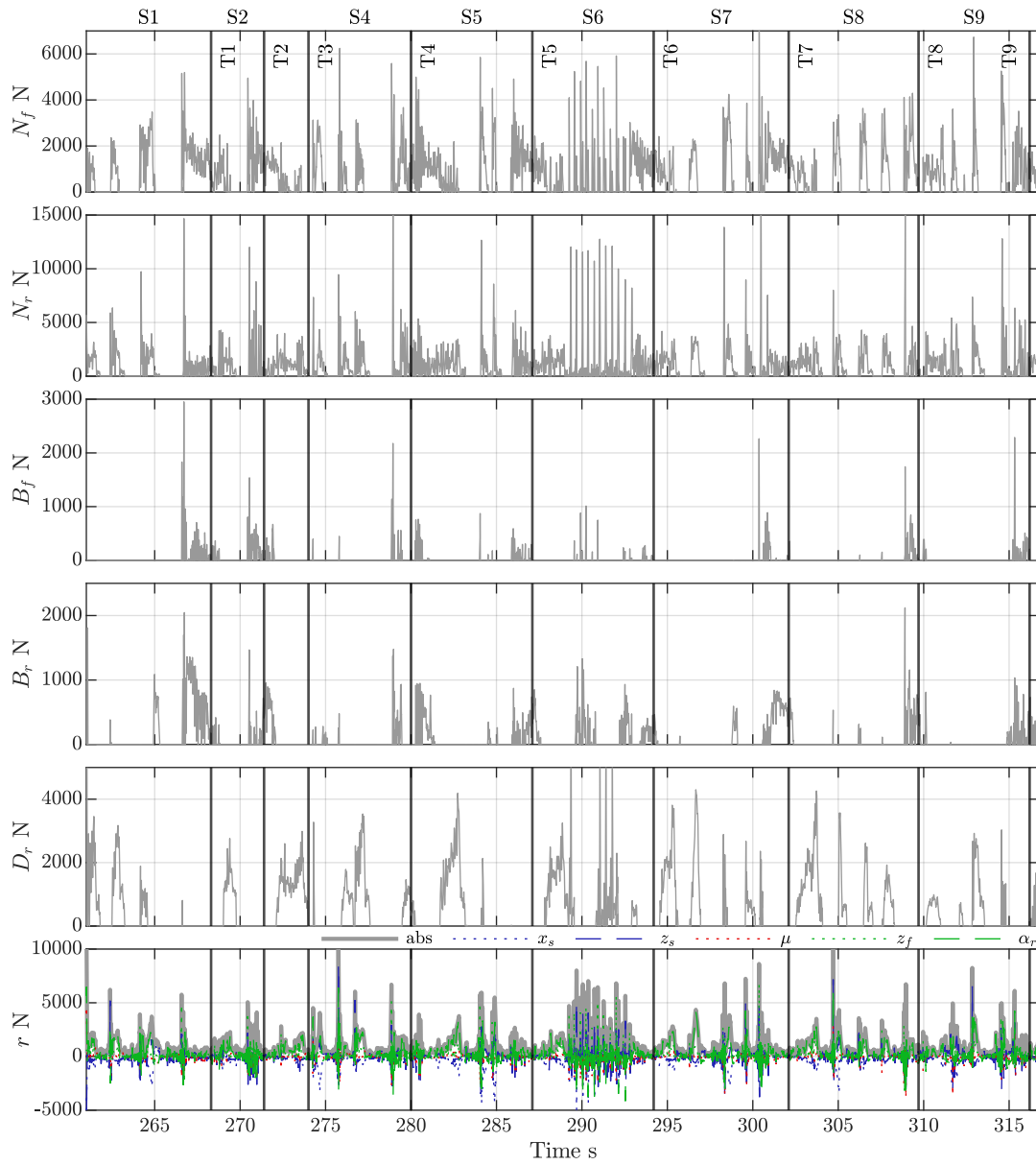
Figure 9: Contact forces on a motocross track estimated from kinematic measurements and the proposed estimator. Zones of jumps, braking, accelerations can be recognized.
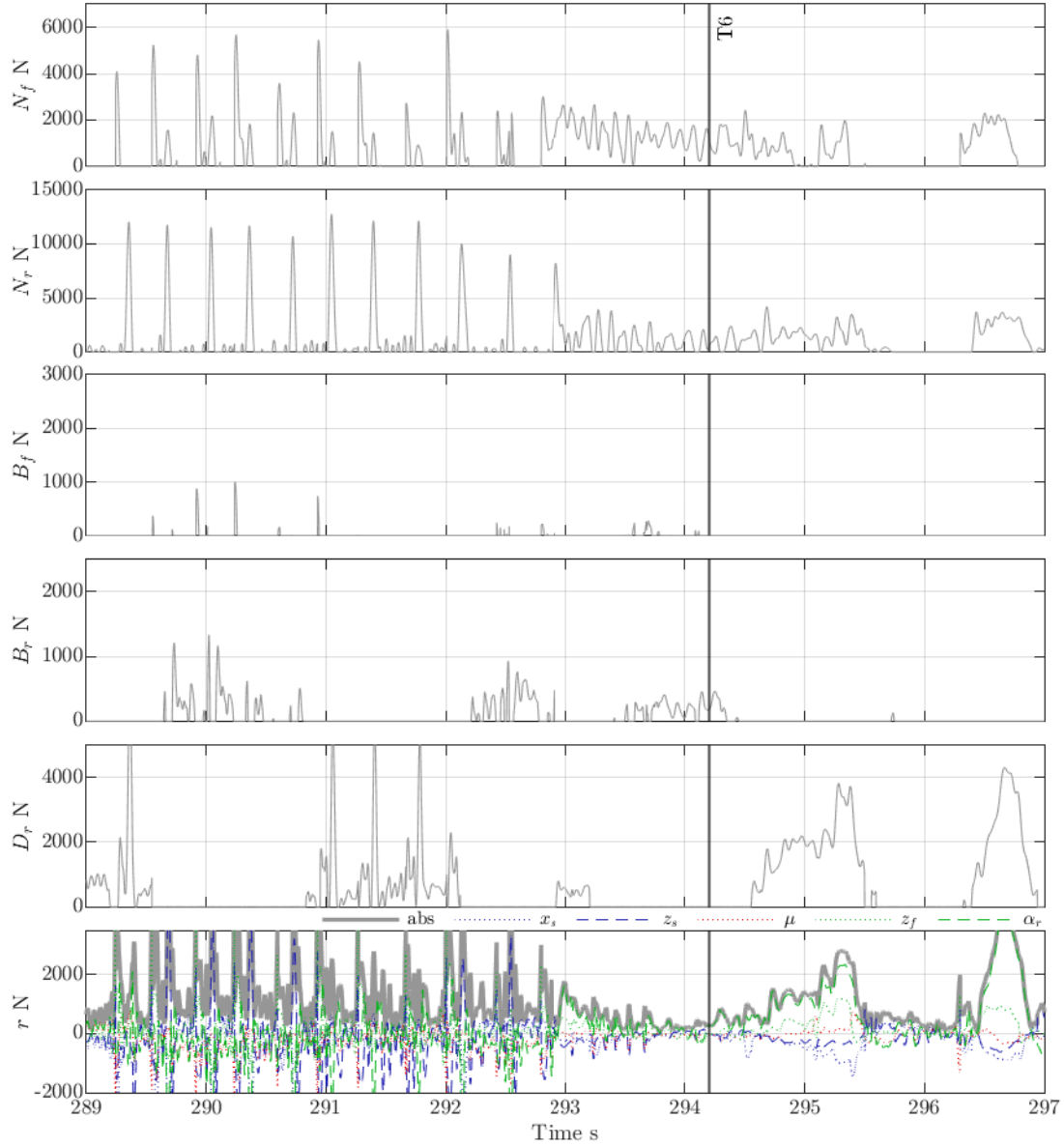
Figure 10: Close up of turn 6. Peaks in normal forces show the *whoops* of S6; absences of rear normal force between $t = 293$ and 294, show detachments of the rear wheel on the braking phase; and rear braking force around $t = 290$ s shows the braking effect of the *whoops* due to the horizontal component of the normal force. Larger residuals on the impact zones and smaller on the turn, shows that the estimator's assumption are in better agreement with reality on the latter.

estimation, another aspect that can be improved is the rider-motorcycle interaction. Nonetheless, the estimator could be exploited to be used as the basis for a controller of a semi-active suspension system, and if lateral dynamic is added, it could also be used for stability control in off-road.

5   Conclusions

In this article we have presented an estimator of contact forces for off-road motorcycles to verify objectively suspension optimisations, avoiding the rider bias. It is based on kinematic measurements and inverse dynamics to overcome the difficulty of direct measurement. Additionally we developed a simple rider model to reproduce the fundamental characteristics of the rider-motorcycle interaction.

Verification against simulation shows that the estimation is in good agreement even with chain tension omission and different rider forces. Experimental tests showed that the estimations vary consistently with the obstacles of the track and therefore can be used as an objective methodology to verify optimisations. Additional information, such as wheel detachments and whoops braking, can also be extracted from the estimations.

Although the estimator have been developed to verify objectively suspension optimisations, it can be used as a basis to develop an on board control system to improve riding safety. Additionally, this methodology can be improved with a measurement system to validate the estimations as well as improving the estimation of rider-motorcycle forces, for example by implementing a rider model based on a vision based system.

Acknowledgements

References

[1] Cossalter, V. (2006) Motorcycle Dynamics, Lulu, .

[2] Gobbi, M., Mastinu, G., and Doniselli, C. (1999) Optimising a car chassis. *Vehicle System Dynamics: International Journal of Vehicle Mechanics and Mobility,* **32**, 149–170.

[3] Gobbi, M., Haque, I., Papalambros, P., and Mastinu, G. (2005) Optimisation and integration of ground vehicle systems. *Vehicle System Dynamics: International Journal of Vehicle Mechanics and Mobility,* **43**, 437–453.

[4] Cossalter, V., Doria, A., Garbin, S., and Lot, R. (2006) Frequency-domain method for evaluating the ride comfort of a motorcycle. *Vehicle System Dynamics: International Journal of Vehicle Mechanics and Mobility,*.

[5] Liguori, C., Paciello, V., Paolillo, A., Pietrosanto, A., and Sommella, P. (2013) Characterization of motorcycle suspension systems: Comfort and handling performance evaluation. In *IEEE Instrumentation and Measurement Technology Conference* pp. 444–449.

[6] van Vliet, M. Computer Aided Analysis and Design of Off-Road Motorcycle Suspensions PhD thesis Concordia University (October, 1983).

[7] Cossalter, V., Doria, A., and Lot, R. (2000) Optimum suspension design for motorcycle braking. *Vehicle System Dynamics: International Journal of Vehicle Mechanics and Mobility,* **54**, 175–198.

[8] Catania, G., Leonelli, L., and Mancinelli, N. (2010) Optimization of the damping parameters of a sport motorcycle. *Information not found,*.

[9] Lozoya-Santos, J., Cervantes-Muñoz, D., Tudon-Martinez, J. C., and Ramirez-Mendoza, R. (2015) Off-Road Motorbike Performance Analysis Using a Rear Semiactive EH Suspension. *Shock and Vibration,*.

[10] Popov, A., Rowell, S., and Meijaard, J. (2010) A review on motorcycle and rider modelling for steering control. *Vehicle System Dynamics: International Journal of Vehicle Mechanics and Mobility,*.

[11] Wang, E. and Hull, M. (1997) A dynamic system model of an off-road cyclist. *Journal of Biomechanical Engineering,* **119**, 248–253.

[12] Wilczynski, H. (1994) A dynamic system model for estimating surface-induced frame loads during off-road cycling. *Journal of Mechanical Design,* **116**, 816 – 822.

[13] Vasquez, F., Lot, R., and Rustighi, E. (2019) Off-Road motorcycle tyre force estimation. In *Proceedings of the 13th International Conference on Recent Advances in Structural Dynamics*.

[14] Acosta, M., Kanarachos, S., and Blundell, M. (2017) Virtual Tyre Force Sensors: An Overview of Tyre Model-based and Tyre Model-less State Estimation Techniques. *Proceedings of the Institution of Mechanical Engineers, Part D: Journal of Automobile Engineering,* **(in press)**, (in press).

[15] Teerhuis, A. P. and Jansen, T. (2012) Motorcycle state estimation for lateral dynamics. *Vehicle System Dynamics,* **50**, 1261–1276.

[16] Slimi, H., Arioui, H., and Mammar, S. (2013) Motorcycle lateral Dynamic Estimation and Lateral Tire-Road Forces Reconstruction Using Sliding Mode Observer. *IEEE Intelligent Transportation System Conference,* pp. 821–826.

[17] Shabana, A. (2005) Dynamics of Multibody Systems, Cambridge University Press, 3rd edition.

[18] Lot, R. and da Lio, M. (2004) A Symbolic Approach for Automatic Generation of the Equations of motion of Multibody Systems. *Multibody System Dynamics,* **12**(2), 147–172.

[19] www.multibody.net. (May, 2019).

[20] Lot, R. and Massaro, M. (2017) A Symbolic Approach to the Multibody Modeling of Road Vehicles. *International Journal of Applied Mechanics,* **09**(05).

[21] www.maplesoft.net. (May, 2019).

[22] Lawson, C. and Hanson, J. (1974) Solving Least-Sqaures Problems, Prentice Hall, .

[23] www.mathworks.com. (May, 2019).

[24] Cheli, F., Mazzoleni, P., Pezzola, M., Ruspini, E., and Zappa, E. (2003) Vision-based measuring system for rider's pose estimation during motorcycle riding.. *Mechanical Systems and Signal Processing,*.

[25] https://youtu.be/NTqFmdJxWmI. (May, 2019).

[26] www.design-simulation.com/wm2d.

Table 3: List of symbols. Sub-index i refers to f or r for front or rear; sub-index j, refers to x and z directions; and sub-index $k \in [1, 2, 3, 4]$, refers to rear wheel, swing arm, chassis, and front wheel, respectively

$\mathbf{A}$	Generalized projection matrix	I_k	Rotational inertia of body k
$\mathbf{A_r}$	Rider force projection matrix	l_r	Distance from body 1 to swing arm main pin
$\mathbf{A_s}$	Suspension force projection matrix	l_s	Distance from swing arm main pin to its CoM
$\mathbf{A_t}$	Tyre force projection matrix	m	Total vehicle mass
$\mathbf{A_w}$	Weights projection matrix	m_k	Mass of body k
$\mathbf{B}$	Generalized weight matrix	m_r	Rider mass
$\mathbf{B_c}$	Relative constraint eq. weight matrix	R_c	Rear wheel sprocket radius
$\mathbf{B_d}$	Relative dynamic eq. weight matrix	R_i	Radius of i wheel
$\mathbf{M}$	Mass matrix	Tn	Turn number n
$\mathbf{W}$	Constraint activation weights matrix	w	Motorcycle wheelbase
$\mathbf{b}$	Generalized known forces vector	w_d	Driving condition weight
$\mathbf{b_1}$	Known forces vector	w_f	Front wheel contact condition weight
$\mathbf{f_r}$	Rider forces vector	w_r	Rear wheel contact condition weight
$\mathbf{f_s}$	Suspension forces vector	x_s	Horizontal displacement of chassis
$\mathbf{f_t}$	Tyre contact forces vector	x_3	Chassis local horizontal axis
$\mathbf{m_v}$	pseudo-mass vector	x_{3h}	Handlebar x-position in chassis frame
$\mathbf{q}$	Motorcycle coordinates vector	x_{3p}	Footpeg x-position in chassis frame
$\mathbf{r}$	Residuals vector	z_f	Fork compression
$\mathbf{\bar{r}}$	Weighted residuals vector	z_r	Shock compression
A_j	Arm forces along direction j	z_3	Chassis local vertical axis
B_i	Braking force on tyre i	z_{3h}	Handlebar z-position in chassis frame
D_i	Driving force on tyre i	z_{3p}	Footpeg z-position in chassis frame
L_j	Leg forces along direction j	z_s	Vertical displacement of chassis
N_i	Normal force on tyre i	α_r	Rear suspension compression angle
T_c	Chain tension	α_{r0}	Nominal rear suspension compression angle
X	Ground forward axis	ϵ	Caster angle
Z	Ground downward axis	μ	Angular displacement of chassis
b	X distance between body 1 and 3	μ_1	Angular displacement of rear wheel
h	Height of chassis CoM	μ_4	Angular displacement of front wheel

Appendix A: Equations of motion

The equations of motion are derived under the four assumptions described in section 2.1, namely, in plane motion, four bodies with five degrees of freedom, standing rider, and contact point under wheel centres.

We derived an equation per degree of freedom using Newton-Euler equations in the following order. First and second equations are sum of forces acting over all bodies along x_s and z_s respectively; third equation, is sum of torques on all bodies around centre of mass of chassis; fourth equation is sum of forces acting on front wheel along z_f; fifth equation is sum of torques acting on rear wheel and swing arm, around the connecting point between body 2 and 3 (P_{23}). Organizing the equations in matrix form, we get

$$\mathbf{M\ddot{q}} + \mathbf{m_v} = \mathbf{A_w}g + \mathbf{A_s f_s} + \mathbf{A_r f_r} + \mathbf{A_t f_t},$$

where the elements on the matrices are the following:

$M_{1,1} = m_4 + m_1 + m_3$

$M_{1,2} = 0$

$M_{1,3} = ((S(\mu + \alpha_{r0} - \alpha_r) - S(\mu + \alpha_{r0}))\,l_r + C(\mu)(h - R_r) + S(\mu)\,b)\,m_1$
$\qquad + (-z_f C(\mu + \epsilon) + C(\mu)(h - R_f) + (b - w)\,S(\mu))\,m_4$

$M_{1,4} = -m_4\,S(\mu + \epsilon)$

$M_{1,5} = -l_r\,m_1\,S(\mu + \alpha_{r0} - \alpha_r)$

$M_{2,2} = m_4 + m_1 + m_3$

$M_{2,3} = ((C(\mu + \alpha_{r0} - \alpha_r) - C(\mu + \alpha_{r0}))\,l_r + (-h + R_r)\,S(\mu) + C(\mu)\,b)\,m_1$
$\qquad + (z_f S(\mu + \epsilon) + (R_f - h)\,S(\mu) + (b - w)\,C(\mu))\,m_4$

$M_{2,4} = -m_4\,C(\mu + \epsilon)$

$M_{2,5} = -l_r\,m_1\,C(\mu + \alpha_{r0} - \alpha_r)$

$M_{3,3} = \big((-2\,C(\alpha_r) + 2)\,{l_r}^2 + ((-2\,R_r + 2\,h)\,S(\alpha_{r0} - \alpha_r) + 2\,C(\alpha_{r0} - \alpha_r)\,b +$
$\qquad (-2\,h + 2\,R_r)\,S(\alpha_{r0}) - 2\,b\,C(\alpha_{r0}))\,l_r + {R_r}^2 - 2\,R_r\,h + b^2 + h^2\big)\,m_1$
$\qquad + \Big({(z_f)}^2 + ((2\,b - 2\,w)\,S(\epsilon) + (2\,R_f - 2\,h)\,C(\epsilon))\,z_f + {R_f}^2$
$\qquad - 2\,R_f\,h + b^2 - 2\,bw + h^2 + w^2\Big)\,m_4 + I_1 + I_2 + I_3 + I_4$

$M_{3,4} = ((R_f - h)\,S(\epsilon) + (w - b)\,C(\epsilon))\,m_4$

$M_{3,5} = \big((C(\alpha_r) - 1)\,{l_r}^2 + ((-h + R_r)\,S(\alpha_{r0} - \alpha_r) - C(\alpha_{r0} - \alpha_r)\,b)\,l_r\big)\,m_1$
$\qquad - I_1 - I_2$

$M_{4,4} = m_4$

$M_{4,5} = 0$

$M_{5,5} = {l_r}^2 m_1 + I_1 + I_2$

$m_{v1,1} = \Big(((C(\mu + \alpha_{r0} - \alpha_r) - C(\mu + \alpha_{r0}))\,l_r + (-h + R_r)\,S(\mu) + C(\mu)\,b)\,{(\dot{\mu})}^2$
$\qquad -2\,(\dot{\alpha}_r)\,C(\mu + \alpha_{r0} - \alpha_r)\,(\dot{\mu})\,l_r + {(\dot{\alpha}_r)}^2\,C(\mu + \alpha_{r0} - \alpha_r)\,l_r\Big)\,m_1$
$\qquad + \Big((z_f S(\mu + \epsilon) + (R_f - h)\,S(\mu) + (b - w)\,C(\mu))\,{(\dot{\mu})}^2 - 2\,C(\mu + \epsilon)\,(\dot{z}_f)\,\dot{\mu}\Big)\,m_4$

$m_{v2,1} = \Big(((-S(\mu + \alpha_{r0} - \alpha_r) + S(\mu + \alpha_{r0}))\,l_r - S(\mu)\,b + (-h + R_r)\,C(\mu))\,{(\dot{\mu})}^2$
$\qquad +2\,(\dot{\alpha}_r)\,S(\mu + \alpha_{r0} - \alpha_r)\,(\dot{\mu})\,l_r - {(\dot{\alpha}_r)}^2\,S(\mu + \alpha_{r0} - \alpha_r)\,l_r\Big)\,m_1$
$\qquad + \Big((z_f C(\mu + \epsilon) + S(\mu)(w - b) + (R_f - h)\,C(\mu))\,{(\dot{\mu})}^2 + 2\,S(\mu + \epsilon)\,(\dot{z}_f)\,\dot{\mu}\Big)\,m_4$

$m_{v3,1} = \Big((2\,S(\alpha_r)\,{l_r}^2 + (2\,S(\alpha_{r0} - \alpha_r)\,b + (-2\,h + 2\,R_r)\,C(\alpha_{r0} - \alpha_r))\,l_r)\,(\dot{\alpha}_r)\,\dot{\mu}$
$\qquad + (-S(\alpha_r)\,{l_r}^2 + (-S(\alpha_{r0} - \alpha_r)\,b + (h - R_r)\,C(\alpha_{r0} - \alpha_r))\,l_r)\,{(\dot{\alpha}_r)}^2\Big)\,m_1$

$$+\left(2\,z_f + (2\,b - 2\,w)\,S\left(\epsilon\right) + (2\,R_f - 2\,h)\,C\left(\epsilon\right)\right)\left(\dot{z}_f\right)\left(\dot{\mu}\right) m_4 + I_1\,\ddot{\mu}_1 + I_4\,\ddot{\mu}_4$$

$$m_{v4,1} = \left(-z_f + (w - b)\,S\left(\epsilon\right) + (h - R_f)\,C\left(\epsilon\right)\right)\left(\dot{\mu}\right)^2 m_4$$

$$m_{v5,1} = \left(-S\left(\alpha_r\right) l_r{}^2 + \left(-S\left(\alpha_{r0} - \alpha_r\right) b + (h - R_r)\,C\left(\alpha_{r0} - \alpha_r\right)\right) l_r\right)\left(\dot{\mu}\right)^2 m_1 - I_1\,\ddot{\mu}_1$$

$$A_{w1,1} = 0$$

$$A_{w2,1} = m_4 + m_1 + m_3$$

$$A_{w3,1} = \left(\left(C\left(\mu + \alpha_{r0} - \alpha_r\right) - C\left(\mu + \alpha_{r0}\right)\right) l_r + (-h + R_r)\,S\left(\mu\right) + C\left(\mu\right) b\right) m_1$$
$$+ \left(z_f S\left(\mu + \epsilon\right) + (R_f - h)\,S\left(\mu\right) + (b - w)\,C\left(\mu\right)\right) m_4$$

$$A_{w4,1} = -m_4\,C\left(\mu + \epsilon\right)$$

$$A_{w5,1} = -l_r\,m_1\,C\left(\mu + \alpha_{r0} - \alpha_r\right)$$

$$\mathbf{A_r} = \begin{bmatrix} -1 & 0 & -1 & 0 \\ 0 & -1 & 0 & -1 \\ A_{r3,1} & A_{r3,2} & A_{r3,3} & A_{r3,4} \\ 0 & 0 & 0 & 0 \\ 0 & 0 & 0 & 0 \end{bmatrix} \qquad \mathbf{A_s} = \begin{bmatrix} 0 & 0 \\ 0 & 0 \\ 0 & 0 \\ -1 & 0 \\ 0 & -1 \end{bmatrix}$$

$$A_{r3,1} = S\left(\mu\right) x_{3p} - C\left(\mu\right) z_{3p}$$
$$A_{r3,2} = C\left(\mu\right) x_{3p} + S\left(\mu\right) z_{3p}$$
$$A_{r3,3} = S\left(\mu\right) x_{3h} - C\left(\mu\right) z_{3h}$$
$$A_{r3,4} = C\left(\mu\right) x_{3h} + S\left(\mu\right) z_{3h}$$

$$\mathbf{A_t} = \begin{bmatrix} -S\left(\mu\right) & -S\left(\mu\right) & -C\left(\mu\right) & -C\left(\mu\right) & C\left(\mu\right) \\ -C\left(\mu\right) & -C\left(\mu\right) & S\left(\mu\right) & S\left(\mu\right) & -S\left(\mu\right) \\ A_{t3,1} & A_{t3,2} & A_{t3,3} & A_{t3,4} & A_{t3,5} \\ C\left(\epsilon\right) & 0 & S\left(\epsilon\right) & 0 & 0 \\ 0 & A_{t5,2} & 0 & A_{t5,4} & A_{t5,5} \end{bmatrix}$$

$$A_{t3,1} = -z_f S\left(\epsilon\right) - b + w$$
$$A_{t3,2} = C\left(\alpha_{r0}\right) l_r - l_r\,C\left(\alpha_{r0} - \alpha_r\right) - b$$
$$A_{t3,3} = z_f C\left(\epsilon\right) - h$$
$$A_{t3,4} = S\left(\alpha_{r0}\right) l_r - l_r\,S\left(\alpha_{r0} - \alpha_r\right) - h$$
$$A_{t3,5} = -S\left(\alpha_{r0}\right) l_r + l_r\,S\left(\alpha_{r0} - \alpha_r\right) + h$$
$$A_{t5,2} = l_r\,C\left(\alpha_{r0} - \alpha_r\right)$$
$$A_{t5,4} = l_r\,S\left(\alpha_{r0} - \alpha_r\right) + R_r$$
$$A_{t5,5} = -l_r\,S\left(\alpha_{r0} - \alpha_r\right) - R_r$$